

Article

The Fast Formation of a Highly Active Homogeneous Catalytic System upon the Soft Leaching of Pd Species from a Heterogeneous Pd/C Precursor

Alexey S. Galushko , Valentina V. Ilyushenkova, Julia V. Burykina , Ruslan R. Shaydullin, Evgeniy O. Pentsak  and Valentine P. Ananikov * 

Zelinsky Institute of Organic Chemistry, Russian Academy of Sciences, 119991 Moscow, Russia

* Correspondence: val@ioc.ac.ru

Abstract: Understanding the interface between soluble metal complexes and supported metal particles is important in order to reveal reaction mechanisms in a new generation of highly active homogeneous transition metal catalysts. In this study, we show that, in the case of palladium forming on a carbon (Pd/C) catalyst from a soluble Pd(0) complex Pd₂dba₃, the nature of deposited particles on a carbon surface turns out to be much richer than previously assumed, even if a very simple experimental procedure is utilized without the use of additional reagents and procedures. In the process of obtaining a heterogeneous Pd/C catalyst, highly active “hidden” metal centers are formed on the carbon surface, which are leached out by the solvent and demonstrate diverse reactivity in the solution phase. The results indicate that heterogeneous catalysts may naturally contain trace amounts of molecular monometallic centers of a different nature by easily transforming them to the homogeneous catalytic system. In line with a modern concept, a heterogenized homogeneous catalyst precursor was found to leach first, leaving metal nanoparticles mostly intact on the surface. In this study, we point out that the previously neglected soft leaching process contributes to high catalyst activity. The results we obtained demand for leaching to be reconsidered as a flexible tool for catalyst construction and for the rational design of highly active and selective homogeneous catalytic systems, starting from easily available heterogeneous catalyst precursors.

Keywords: leaching; catalysis; solvent; dynamic transformations; cocktail of catalysts; carbon materials; electron microscopy; mass spectrometry



Citation: Galushko, A.S.; Ilyushenkova, V.V.; Burykina, J.V.; Shaydullin, R.R.; Pentsak, E.O.; Ananikov, V.P. The Fast Formation of a Highly Active Homogeneous Catalytic System upon the Soft Leaching of Pd Species from a Heterogeneous Pd/C Precursor. *Inorganics* **2023**, *11*, 260. <https://doi.org/10.3390/inorganics11060260>

Academic Editors: Axel Klein, S. Masoud Nabavizadeh and Fatemeh Niroomand Hosseini

Received: 26 May 2023
Revised: 13 June 2023
Accepted: 15 June 2023
Published: 19 June 2023



Copyright: © 2023 by the authors. Licensee MDPI, Basel, Switzerland. This article is an open access article distributed under the terms and conditions of the Creative Commons Attribution (CC BY) license (<https://creativecommons.org/licenses/by/4.0/>).

1. Introduction

Transition metal catalysts play an important role in organic synthesis, polymer science, the production of biologically active compounds, and industry developments [1–3]. The synthesis and modification of monometallic nanocatalysts [4–11], bimetallic nanocatalysts [12–15], and mixed metal-nonmetallic nanocatalysts [16–18] are actively investigated in recent years. In particular, heterogeneous carbon-supported metal nanoparticle catalysts (M/C) have been applied in the fine chemical industry [19], energy research [20], and metal-catalyzed reactions in organic synthesis [21–23]. Indeed, palladium deposited on a carbon support is one of the most commonly used catalysts. Carbon materials are inexpensive, widely available, and easy to manufacture and recycle; they can be produced from biomass; they have a large specific surface area; and they represent efficient support for metal catalyst particles [24].

Recent studies have shown that there are no clear boundaries between homogeneous and heterogeneous catalysis [25–29]. The application of a heterogeneous catalyst often leads to the formation of soluble metal complexes, while the use of a homogeneous catalyst can result in the deposition of metal nanoparticles or the precipitation of metal black [27,28]. The removal of metal from the surface of the support using the reaction mixture (leaching) is now well known in a number of catalytic processes [29]. Even minor contamination of

the reaction system with palladium can significantly affect catalytic activity [30]. A new wave in the research on M/C catalysts was initiated by investigating the role of leaching in Pd-catalyzed cross-coupling, the Mizoroki–Heck reaction, C–H activation, etc. [31].

Leaching usually takes place at higher temperatures and leads to modifications in the catalyst and the contamination of the reaction system's liquid phase with metals [32–35]. Catalytic sites formed during leaching often exhibit high activity, allowing the reaction to be carried out with higher turnover number/turnover frequency (TON/TOF) values and a greater resistance to functional groups in reagent molecules compared to purely heterogeneous catalytic systems. These centers are observed in the form of mono- and bimetallic complexes, nanoparticles, or clusters, which can exist in equilibrium or transform into each other. This behavior was described as a “cocktail”-type catalysis [27,29]. Important studies on the dynamic behavior of catalysts and the mechanisms of active site formation have been carried out by several research groups [36–53]. A dedicated focus on the application of leaching in the case of supported catalysts was also made [54–57]. de Bellefon and co-workers conducted a detailed literature review on mechanistic studies pertaining to the Suzuki–Miyaura reaction and showed that there is evidence supporting a homogeneous mechanism for this reaction. [25]. In this case, the applied palladium mainly acts as a reservoir for active palladium particles resulting from leaching. Then, the heterogeneous catalyst gradually loses its activity due to a decrease in the total palladium content. It should be noted that leaching is not the only reason for the loss of catalyst activity. For example, Kiwi-Minsker and co-workers showed that the loss of catalytic activity can be caused by the sorption of Suzuki–Miyaura reaction products [58]. Washing the catalyst with an organic solvent while stirring promotes the regeneration of the catalyst. The solvent is an important part of the catalytic systems and forms the medium for the reaction proceed. Often, the impact of the solvent during the reaction is neglected, so it is considered to be a stable medium, within which the chemical reaction proceeds. Ignoring the influence of the solvent may prevent important effects of the system from being revealed. For example, Wang, Dai, and co-workers have reported a significant effect of solvent choice on the performance of the catalyst based on zinc and activated carbon [59].

Previously, it was shown that metal deposition from the tris(dibenzylideneacetone)dipalladium(0) (Pd_2dba_3) complex in chloroform has the ability to produce palladium nanoparticles and form practically significant highly active Pd/C supported catalysts (Figure 1A) [23,60,61]. As typically assumed, during the preparation of the catalyst, the Pd_2dba_3 complex decomposes with the formation of palladium nanoparticles in solution, as well as with the release of free dibenzylideneacetone (dba). Palladium particles are strongly attached to the carbon substrate due to their high binding energy [62]. The dba ligand remains in the solvent, within which the complex decomposes to form Pd nanoparticles [60]. Our recent studies have shown that both nanoparticles and also individual surface palladium atoms are formed during catalyst preparation using this method [63]. Individual palladium atoms are easily leached by reagents from the surface of the carbon support into the reaction mixture. It has also been found that individual palladium atoms subjected to leaching play a key role in the catalysis of Suzuki–Miyaura and Mizoroki–Heck reactions. Individual palladium atoms, like other surface monatomic palladium-containing centers, are usually not visible on regular electron microscope images due to their small size and require a special approach and tools for the investigation. The catalytic behavior of monatomic metal centers of various metals is actively studied in many reaction systems, mainly using high-resolution electron microscopy and X-ray absorption spectroscopy [64–66].

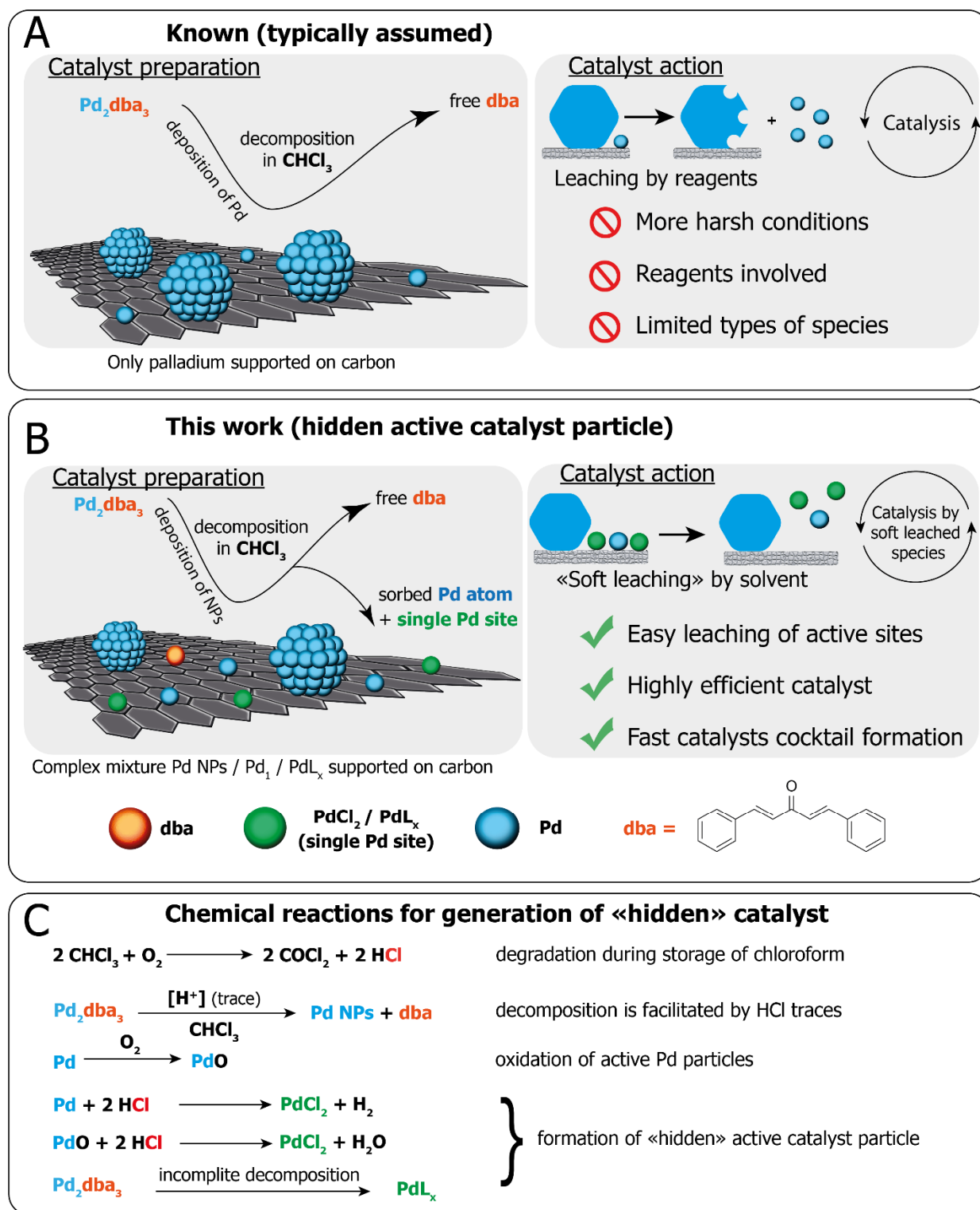


Figure 1. (A) Typical picture of Pd_2dba_3 complex decomposition to obtain a Pd/C catalyst, which consists of the formation of only metal particles (nanoparticles, clusters, and single atoms). (B) The complete process, including the formation of “hidden”, easily leached, and highly catalytically active species disclosed here, during the formation of a Pd/C catalyst from Pd_2dba_3 , is demonstrated in this study. (C) Corresponding chemical reactions.

In this study, we consider an additional way of studying systems in which monometallic centers are formed (Figure 1B), the leaching of which promotes the highly efficient catalysis of organic reactions. The combination of electrospray ionization mass spectrometry (ESI-MS) and scanning electron microscopy (SEM) was applied to carry out a mechanistic study. The “hidden” easily soluble on-surface metal-containing complexes, though previously not considered, were found to be highly active in the catalysis of the Mizoroki–Heck reaction.

2. Results and Discussions

Practically popular, fast, and convenient catalyst preparation is based on the decomposition of the Pd₂dba₃ complex in chloroform in the presence of a carbon material [60]. This palladium complex is unstable in solution and rapidly decomposes into Pd atoms, clusters, nanoparticles, and a free ligand (dba) [23,63]. These palladium particles were deposited on a carbon support. After simply washing them with a solvent (acetone or chloroform), the catalyst was completely ready for use.

It is very convenient to control the completeness of the catalyst formation and decomposition of the complex by changing the color of the chloroform solution. At the initial stage, the dissolved complex has a saturated burgundy color, but as it decomposes and metal particles precipitate, the color disappears, and the final solution has a slightly yellow color due to the released ligand (dba). NMR spectroscopy is a useful analytic method that is used to register the signals corresponding to the Pd₂dba₃ complex (Figure 2A) and monitor the release of free dba (Figure 2B).

The approach is universal and makes it possible to deposit palladium on various supports, such as graphite (Figure 2C) or nanotubes (Figure 2D). It is important to note that the rate of decomposition of the complex not only depends on the temperature (the higher the temperature, the faster the decomposition), but also on the acidity of the medium. It was noted that when stored for some time, the chloroform used as a solvent promotes the faster decomposition of the complex, while in chloroform, freshly distilled over calcium hydride, decomposition occurs more slowly at the same temperature. It is known that the long-term storage of chloroform is accompanied by its decomposition with the formation of hydrogen chloride (Figure 1C) [67]. The formed hydrogen chloride contributes to the decomposition of the complex, accelerating the process of metal Pd particle formation [23].

In parallel with the above, the electronic structure of the obtained palladium nanoparticles was studied since it is an important parameter for catalyst efficiency [68]. When palladium is deposited from the Pd₂dba₃ complex in an inert atmosphere, the majority of palladium should be in a zerovalent state. However, in this study, XPS analysis showed that the nanoparticles were very rapidly oxidized in air with the formation of an oxide phase (Figures S1 and S2). The PdO to Pd(0) ratios were 51% and 24% for the palladium on multiwalled carbon nanotube (Pd/MWCNT) and Pd/graphite catalysts, respectively. Interestingly, the type of carbon support strongly influenced the proportion of palladium oxide, probably due to differences in the average diameters of nanoparticles, which, according to scanning electron microscopy, were approximately 2 and 6 nm for MWCNTs and graphite, respectively.

We assumed that dissolved hydrogen chloride, which caused the accelerated decomposition of the complex, is able to react with Pd(0) and freshly formed palladium oxide, making the formation of palladium chloride possible. Palladium chloride is a common highly active catalyst [69], so its trace amounts can have a significant effect on catalysis, the activity of which was previously attributed exclusively to deposited metal nanoparticles.

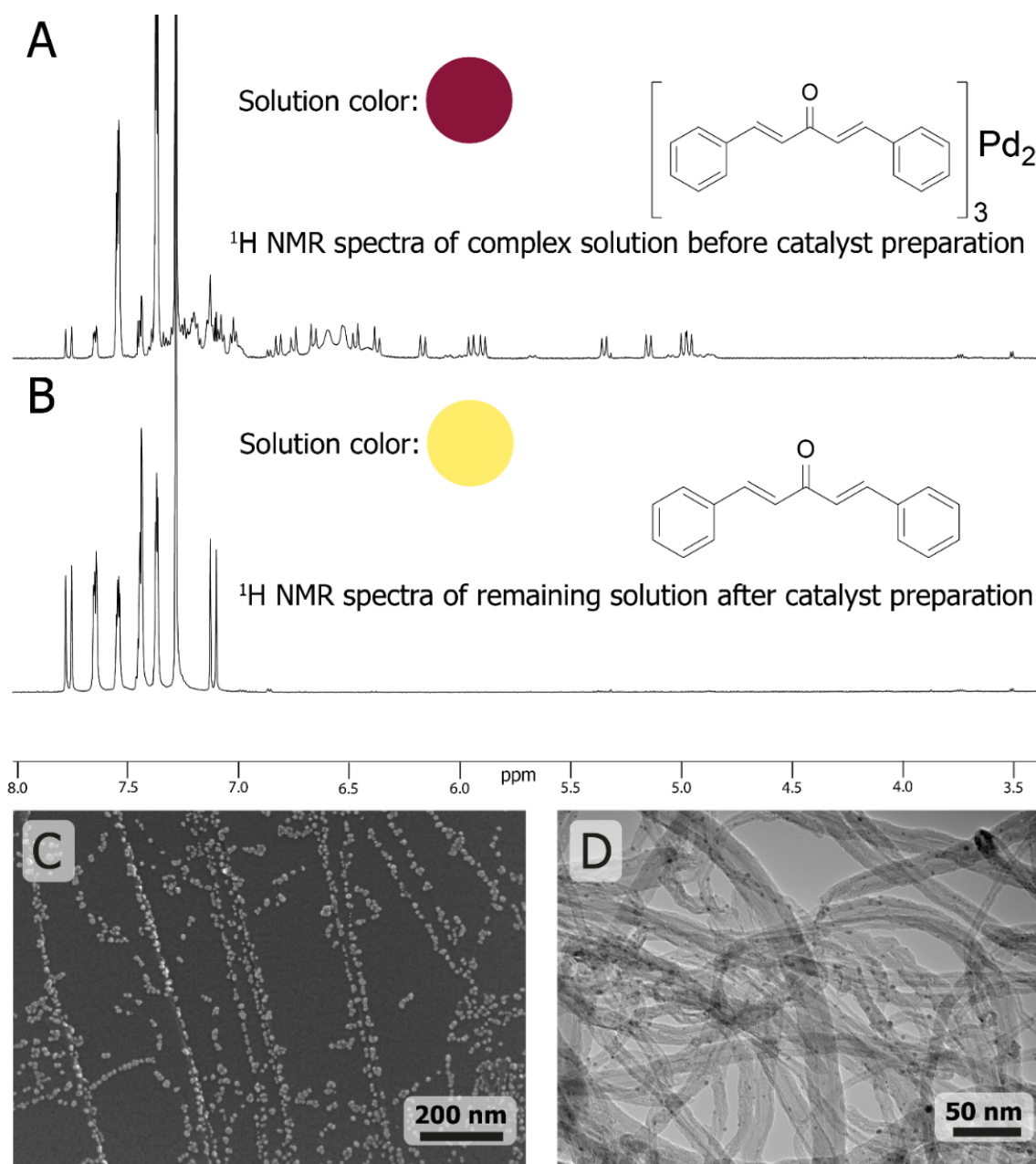


Figure 2. (A) ^1H NMR spectra of a solution containing the Pd_2dba_3 complex in CDCl_3 before and (B) after decomposition of the complex. (C) SEM images of palladium nanoparticles obtained by this method on graphite and (D) TEM images of palladium nanoparticles deposited on carbon nanotubes.

A specially designed experiment was carried out to test the hypothesis of palladium chloride presence in the catalyst. Palladium particles were deposited on a graphite rod, as described above (Figure 3A,D). Next, several parts with an area of approximately $1.3 \mu\text{m}^2$ were selected so that all the nanoparticles in the area were clearly visible. The graphite was then heated in pure *N,N*-dimethylformamide (DMF) at 120°C for 1 h, and the ESI-MS spectra of the resulting solution were recorded in both positive and negative ion modes. Indeed, a PdCl_2^- signal was detected ($m/z = 177.8475$), as well as a dba signal ($m/z = 235.1125$). A re-examination of previously selected areas using SEM did not reveal noticeable changes in surface morphology (Figure 3B,E). A detailed methodology for tracking selected areas of the catalyst is described in [63]. Previously deposited palladium nanoparticles remained in their places, which indicates the great strength of the bond

between palladium and graphite, even under such harsh conditions after 2 h (Figure 3C,F), as well as the preservation of their morphology.

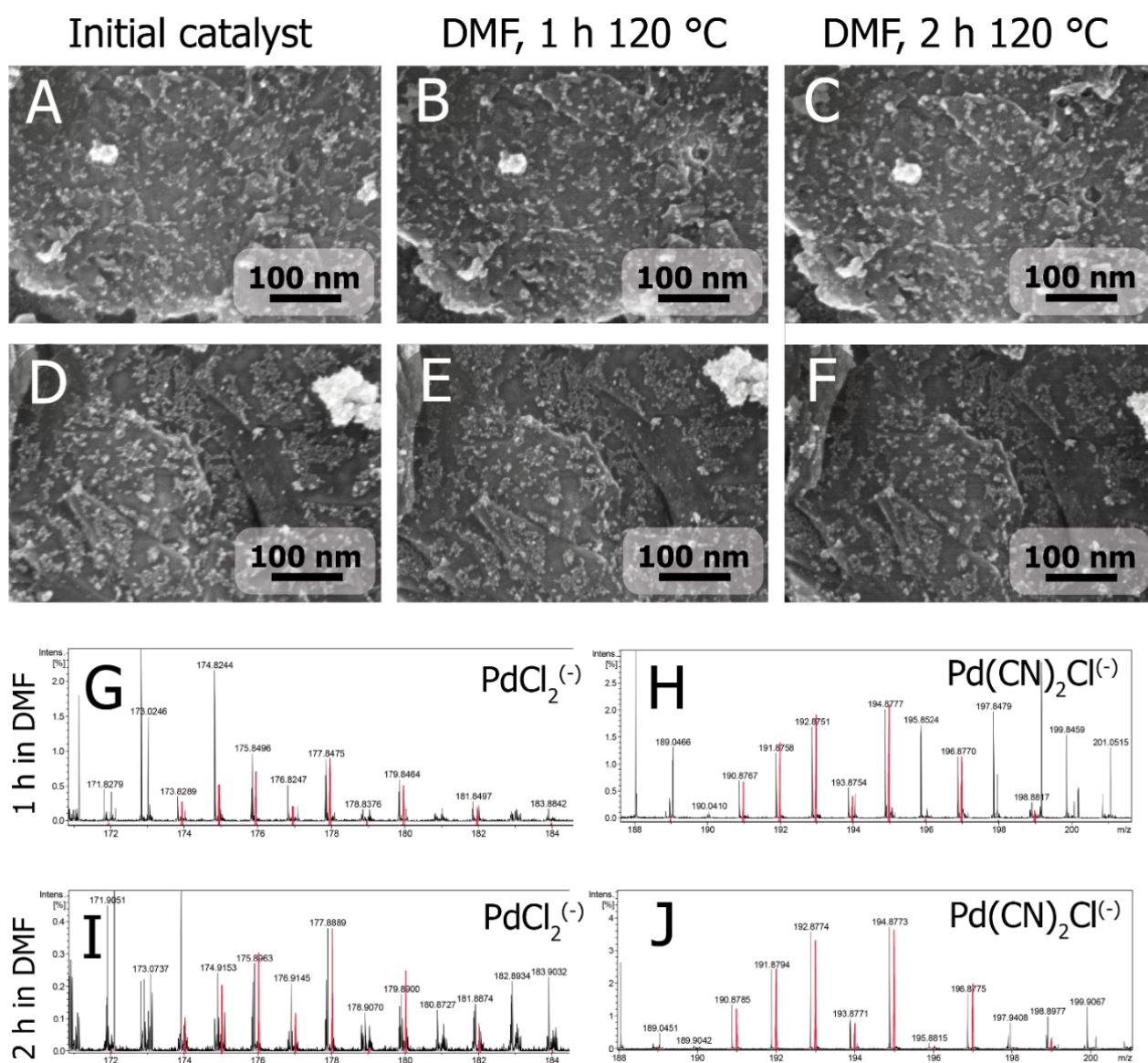


Figure 3. Sequential capture via SEM of the same areas of the Pd/graphite catalyst (A,D) at 1 h (B,E) and 2 h (C,F) in pure DMF at 120 °C. Mass spectra of palladium chloride were recorded at 1 h (G) and 2 h (I), and mass spectra of the cyanide–chloride complex of palladium were recorded at 1 h (H) and 2 h (J) in pure DMF at 120 °C. The red lines show the simulated theoretical spectra for the registered ions.

An unexpected result was the registration of ions with m/z values of 194.8773, 131.9063, 157.9146, 158.9168, and others (Figures S6–S9 and S12–S16), which correspond to palladium cyanide complexes and mixed chloride–cyanide complexes. With time, the intensity of PdCl₂[−] in the mass spectra decreased (Figure 3G,I), while the relative intensity of the [Pd(CN)₂Cl][−] ion increased (Figure 3H,J). It is likely that palladium chloride begins to react with the solvent (DMF) at high temperatures, resulting in the formation of cyanide ions and the displacement of chlorine, and such a Pd-catalyzed conversion of DMF to cyanide is well known in the literature [70]. Surface single atoms of palladium are highly coordinately unsaturated, and therefore are highly active in various reactions [71–73]. One of the ways of forming some palladium-containing particles can be the interaction of highly active

single palladium atoms with a solvent and impurities in it, which can be present in trace amounts, even in very pure reagents.

Thus, from the surface of the catalyst, obtained by the decomposition of the Pd₂dba₃ complex, many unexpected (“hidden”) species were leached out, which can have a significant effect on catalysis. A special experiment was carried out to test the catalytic activity of the leached hidden species. Within 60 min, the active species were leached out of the catalyst 1 wt.% Pd/C (C = MWCNT or graphite) at 140 °C in pure DMF. During this time, the amount of leached metal measured by ICP-AES was 0.54% of the total palladium content on the substrate in the case of nanotubes and 20.38% in the case of graphite. ESI-MS analysis on the solution showed that eight types of palladium-containing ions were detected in the negative ion mode and six types were detected in the positive ion mode in the case of Pd/MWCNTs (Figures S3 and S4). However, in the case of Pd/graphite, eight palladium-containing ions were detected in the negative ion mode (Figure S5), but were not observed in the positive ion mode. Then, the reagents of the Heck reaction were added to the resulting solutions (Table 1). As a result, NMR analysis showed the formation of products in all cases, confirming the catalytic activity of palladium particles leached by the solvent. The highest conversion was achieved for the solution with the lowest content (by ICP-AES) of leached palladium, but the highest diversity of palladium species (by ESI-MS) obtained from the Pd/MWCNT catalyst. These results are very consistent and complement a recent study in which we showed the extraordinary activity of individual Pd/C catalyst particles [74].

Table 1. A comparison of catalyst activity levels in the Mizoroki–Heck reaction and the amount of leached palladium from Pd/MWCNTs and Pd/graphite.

Catalyst	Fraction of Leached Pd in Pure DMF in 1 h at 140 °C	Number of Pd-Containing Ions Detected by ESI-MS After Soft Leaching	NMR Conversion of ArI to Product in 5 h, Catalyzed by Only Leached Pd
Pd/MWCNTs	0.54%	8 (anions) + 6 (cations)	30%
Pd/graphite	20.38%	8 (anions)	10%

In addition, an experiment was carried out to detect palladium complexes 2 h after the start of the Mizoroki–Heck reaction. The solution was found to contain an oxidative addition complex [Pd(C₆H₄NO₂)I₂][−] with *m/z* = 481.7381 (Figure S10). In addition, we observed an ion with *m/z* = 391.8017, which corresponds to the formula [Pd(C₆H₄NO₂)ICl][−] (Figure S11). Since palladium chloride (PdCl₂) was not used in the preparation of the catalyst, the appearance of palladium containing complexes [PdCl_n] particles can only be explained by the formation of PdCl₂ from Pd₂dba₃ in chloroform during the preparation of the catalyst. This is an interesting example of interhalide complexes found in the present study. The role of these particles in the catalytic cycle requires further detailed investigation.

The presence of dba (Figure S17) in the obtained solution was found by the ESI-MS of leachable particles from Pd/C (C = MWCNT). Most likely, the incompletely decomposed Pd₂dba₃ complex can be adsorbed by carbon support (Figure 1B). Heterogenized Pd(dba)_x on a support (PdL_x/C) cannot be detected using conventional electron microscopy, such as single Pd atoms, unlike Pd nanoparticles. In this case, PdL_x/C can easily leach out into the solution when a solvent is added. Thus, the observed free dba signal in the ESI-MS spectrum may also be attributed to a product of the desorption and thermal decomposition of residual Pd(dba)_x particles in the spray cone of the mass spectrometer.

In the studied case, leaching occurred simply after the nanoscale Pd/C catalyst made contact with the solvent (without the addition of any reagents). In contrast, it is typically assumed that leaching involves the oxidative addition of aryl halides or other chemical reactions. This may be the reason why leaching mediated only with soft solvents was previously overlooked.

3. Materials and Methods

General information. Pd/C catalysts were prepared using a previously published protocol [60,63]. In the case of a graphite bar (25 × 5 × 2 mm), palladium was deposited from 0.4 mg of Pd₂dba₃. DMF (anhydrous) and other chemicals were obtained from Sigma-Aldrich (Merck KGaA, Darmstadt, Germany) and Acros Organics (Thermo Fisher Scientific, Geel, Belgium) without additional purification. The samples for the ESI-MS experiments were prepared in 1.8 mL glass vials with screw-top caps fitted with Teflon-lined septa (Agilent Technologies, Santa Clara, CA, USA). NMR measurements were performed using a Bruker Fourier 300HD spectrometer (Bruker Daltonik GmbH, Bremen, Germany) operating at 300.1 MHz and Bruker Avance 600 (Bruker Daltonik GmbH, Bremen, Germany) at 600 MHz for ¹H nuclei. ¹H NMR chemical shifts were reported relative to the solvent signals as internal standards. All measurements were performed at room temperature.

Mizoroki–Heck reaction. In total, 10.6 mg of 1 wt.% Pd/C (0.1 mol.% Pd) and 4 mL of DMF were heated at 140 °C for 1 h. Then, the mixture was filtered to separate the solid catalyst and the liquid phase. A test tube with a magnetic stir bar and a previously prepared liquid phase was loaded with 1-iodo-4-nitrobenzene (249 mg, 1 mmol), styrene (115 µL, 1 mmol), and triethylamine (140 µL, 1 mmol). The reaction mixture was stirred at 140 °C, the yield was measured by ¹H NMR, and the samples for ESI-MS analyses were prepared.

ESI-MS study. High-resolution mass spectra were recorded on a Bruker maXis QTOF (Bruker Daltonik GmbH, Bremen, Germany) (tandem quadrupole/time-of-flight mass analyzer) mass spectrometer equipped with an electrospray ionization (ESI) ion source. The *m/z* scanning range was 90–1200. The external calibration of the mass scale was carried out using a low-concentration calibration solution “Tuning mix” (Agilent Technologies, Santa Clara, CA, USA). The samples were injected using a 500 µL Hamilton RN 1750 syringe (Hamilton Bonaduz AG, Bonaduz, GR, Switzerland). The measurements were carried out in positive ion mode (+) (grounded spray needle, 4500 V high-voltage capillary; HV end plate offset: –500 V) and in negative ion mode (–) (grounded spray needle, +4000-V high-voltage capillary; HV end plate offset: –500 V). Nitrogen was applied as the nebulizer gas (1.0 bar) and dry gas (4.0 L/min, 200 °C). The data were processed using Bruker Data Analysis 4.0 software.

ESI-MS study of leaching using DMF. The catalyst (10.6 mg) and DMF (2 mL) were placed into a 5 mL glass vial. The mixture was stirred at room temperature on a bioSan TS-100 thermal shaker for 10 min; an aliquot (100 µL) was taken, centrifuged, and injected into the ionization source, and mass spectra were recorded in positive and negative modes.

ESI-MS study of leaching in reaction mixtures. Aliquots of the reaction mixture (100 µL) were taken after 2 h of heating with a syringe and filtered through a polyvinylidene fluoride (PVDF) filter. After that, 5 µL of filtrate was taken, diluted in 1 mL of DMF, and then centrifuged and injected into the ionization source.

TEM study. A standard copper TEM grid (200 mesh) with carbon film was immersed in a colloid of suspended catalyst particles in isopropanol. Then, it was dried in air. Electron microscopic observations were carried out using a Hitachi HT7700 transmission electron microscope (Hitachi, Ltd., Tokyo, Japan) operating in bright field mode at an accelerating voltage of 100 kV.

SEM study. Before measurements, the samples were mounted on a 25 mm aluminum specimen stub and fixed with conductive graphite adhesive tape or a special holder. Sample morphology was studied under native conditions to exclude metal coating surface effects. The observations were carried out using a Hitachi SU8000 field-emission scanning electron microscope (FE-SEM) (Hitachi, Ltd., Tokyo, Japan). Images were acquired in secondary

electron mode at an accelerating voltage of 20 kV and at a working distance of 8–10 mm. A slight deterioration in the image quality is associated with the sorption of DMF and the carbonization of its traces under the action of the electron beam.

ICP-AES experiments. Aliquots of the reaction mixture (2 mL) were taken after 6 h of heating with a syringe and filtered through a PVDF filter. The following settings were used: plasma power—1.2 kW, plasma flow—12 L \times min⁻¹, axial flow—1.0 L \times min⁻¹, and nebulizer flow—0.75 L \times min⁻¹. A measurement time of 15 s (5 replicas of 3 s) was also set. To prepare the calibration solutions, a monoelement solution of Pd ions from High Purity Standards (USA) 1 g \times L⁻¹ in 5% HCl was used.

XPS study. X-ray photoelectron spectra were collected at an ESCA unit of the NanoPES synchrotron station (Kurchatov Synchrotron Radiation Source, National Research Center Kurchatov Institute Moscow, Russia), equipped with a high-resolution SPECS Phoibos 150 (SPECS Surface Nano Analysis GmbH, Berlin, Germany) hemispherical electron energy analyzer with a monochromatic Al X-ray source (with an excitation energy of 1486.61 eV and $\Delta E = 0.2$ eV).

4. Conclusions

To summarize, the experiments suggest that the formation of a supported catalyst is a more complicated process than previously thought. The solvent used affects the final system, which leads to the formation of a “hidden” highly active species acting as homogeneous catalytic centers in the liquid phase. It is important to mention that such a “hidden” species, in addition to the already-known individual Pd atoms, may contain palladium chloride, residual intermediates of the decomposition of Pd₂dba₃ and cyanides, as well as palladium chloride–cyanide complexes formed after interacting with the solvent (DMF) of the reaction mixture.

To obtain a deeper understanding of the operation of the catalyst, the activity of hidden easily leached particles was addressed and separately studied. For this study, a hybrid experiment was carried out alongside parallel ESI-MS analysis on solvent-leached catalyst species and SEM analysis on the exact same surface area. The high activity of easily solvent leached out “hidden” palladium particles was shown. The results obtained provide additional insight for the phenomena described recently with the specific participation of single-atom catalyst (SAC) centers in catalysis [63,66,73]. It was found that the concentration of palladium in the considered catalytic system does not correlate with the activity of this system. Using the example of the Mizoroki–Heck reaction, it was shown that the greater the number of individual palladium-containing species recorded by ESI-MS, the higher the activity of this catalyst, even at very low total concentrations of palladium.

Supplementary Materials: The following supporting information can be downloaded at: <https://www.mdpi.com/article/10.3390/inorganics11060260/s1>. Figure S1: XPS spectrum of palladium. Figure S2: XPS spectrum of palladium. Figure S3: Full ESI-MS spectra in negative ion mode: ions formed in 1 wt.% Pd/MWCNTs suspension in DMF. Figure S4: Full ESI-MS spectra in positive ion mode: ions formed in 1 wt.% Pd/MWCNTs suspension in DMF. Figure S5: Full ESI-MS spectra in negative ion mode: ions formed in 1 wt.% Pd/graphite suspension in DMF. Figure S6: ESI-MS spectra in negative ion mode: ions formed in Pd/graphite rod (1 h of heating). Experimental (top) and calculated (bottom) spectra of [PdCl₂]⁻. Figure S7: ESI-MS spectra in negative ion mode: ions formed in Pd/graphite rod (2 h of heating). Experimental (top) and calculated (bottom) spectra of [PdCl₂]⁻. Figure S8: ESI-MS spectra in negative ion mode: ions formed in Pd/graphite rod (1 h of heating). Experimental (top) and calculated (bottom) spectra of [PdCl(CN)₂]⁻. Figure S9: ESI-MS spectra in negative ion mode: ions formed in Pd/graphite rod (2 h of heating). Experimental (top) and calculated (bottom) spectra of [PdCl(CN)₂]⁻. Figure S10: ESI-MS spectra in negative ion mode: [Pd(C₆H₄NO₂)₂]⁻ found in reaction mixture in the Mizoroki-Heck reaction with leached palladium species to DMF. Figure S11: ESI-MS spectra in negative ion mode: [Pd(C₆H₄NO₂)₂]⁻ found in Mizoroki-Heck reaction with leached palladium species to DMF. Figure S12: ESI-MS spectra in negative ion mode: Experimental (top) and calculated (bottom) spectra of [Pd(CN)₂]⁻. Figure S13: ESI-MS spectra in negative ion mode: Experimental (top) and calculated (bottom) spectra of

[Pd(CN)₂H][−]. Figure S14: ESI-MS spectra in negative ion mode: Experimental (top) and calculated (bottom) spectra of [Pd(CN)₃][−]. Figure S15: ESI-MS spectra in negative ion mode: Experimental (top) and calculated (bottom) spectra of [PdO(CN)₃][−]. Figure S16: ESI-MS spectra in negative ion mode: Experimental (top) and calculated (bottom) of [Pd(CN)][−]. Figure S17: ESI-MS spectra in positive ion mode: Experimental (top) and calculated (bottom) of dibenzylideneacetone found in mixture Pd/MWCNT in DMF.

Author Contributions: Conceptualization, V.P.A.; investigation, A.S.G., V.V.I., J.V.B., R.R.S. and E.O.P.; methodology A.S.G., V.V.I. and J.V.B.; supervision, V.P.A.; writing—original draft, A.S.G. and V.P.A. All authors have read and agreed to the published version of the manuscript.

Funding: This research received no external funding.

Data Availability Statement: Data are contained in the article and Supplementary Materials.

Conflicts of Interest: There are no conflict to declare.

References

1. Rana, S.; Biswas, J.P.; Paul, S.; Paik, A.; Maiti, D. Organic synthesis with the most abundant transition metal-iron: From rust to multitasking catalysts. *Chem. Soc. Rev.* **2021**, *50*, 243–472. [[CrossRef](#)] [[PubMed](#)]
2. Fu, L.; Chen, Q.; Nishihara, Y. Recent Advances in Transition-metal-catalyzed C-C Bond Formation via C(sp²)-F Bond Cleavage. *Chem. Rec.* **2021**, *21*, 3394–3410. [[CrossRef](#)] [[PubMed](#)]
3. Arisawa, M.; Yamaguchi, M. Rhodium-Catalyzed Synthesis of Organosulfur Compounds Involving S-S Bond Cleavage of Disulfides and Sulfur. *Molecules* **2020**, *25*, 3595. [[CrossRef](#)] [[PubMed](#)]
4. Zhang, S.; Li, J.; Xia, Z.; Wu, C.; Zhang, Z.; Ma, Y.; Qu, Y. Towards highly active Pd/CeO₂ for alkene hydrogenation by tuning Pd dispersion and surface properties of the catalysts. *Nanoscale* **2017**, *9*, 3140–3149. [[CrossRef](#)] [[PubMed](#)]
5. Cao, F.; Song, Z.; Zhang, Z.; Xiao, Y.-S.; Zhang, M.; Hu, X.; Liu, Z.-W.; Qu, Y. Size-Controlled Synthesis of Pd Nanocatalysts on Defect-Engineered CeO₂ for CO₂ Hydrogenation. *ACS Appl. Mater. Interfaces* **2021**, *13*, 24957–24965. [[CrossRef](#)]
6. Zhou, J.; Hou, W.; Liu, X.; Astruc, D. Pd, Rh and Ru nanohybrid-catalyzed tetramethyldisiloxane hydrolysis for H₂ generation, nitrophenol reduction and Suzuki–Miyaura cross-coupling. *Inorg. Chem. Front.* **2022**, *9*, 1416–1422. [[CrossRef](#)]
7. Liu, Y.; Lopes, R.P.; Lüdtke, T.; Di Silvio, D.; Moya, S.; Hamon, J.-R.; Astruc, D. “Click” dendrimer-Pd nanoparticle assemblies as enzyme mimics: Catalytic *o*-phenylenediamine oxidation and application in colorimetric H₂O₂ detection. *Inorg. Chem. Front.* **2021**, *8*, 3301–3307. [[CrossRef](#)]
8. Wang, W.; Chamkina, E.S.; Guisasola Cal, E.; Di Silvio, D.; Moro, M.M.; Moya, S.; Hamon, J.-R.; Astruc, D.; Shifrina, Z.B. Ferrocenyl-terminated polyphenylene-type “click” dendrimers as supports for efficient gold and palladium nanocatalysis. *Dalton Trans.* **2021**, *50*, 11852–11860. [[CrossRef](#)]
9. Costa, N.J.S.; Vono, L.L.R.; Wojcieszak, R.; Teixeira-Neto, E.; Philippot, K.; Rossi, L.M. One-pot organometallic synthesis of alumina-embedded Pd nanoparticles. *Dalton Trans.* **2017**, *46*, 14318–14324. [[CrossRef](#)]
10. Zhang, M.; Zou, Y.; Zhang, S.; Qu, Y. Modulated electronic structure of Pd nanoparticles on Mg(OH)₂ for selective benzonitrile hydrogenation into benzylamine at a low temperature. *Inorg. Chem. Front.* **2022**, *9*, 4899–4906. [[CrossRef](#)]
11. Gómez-Villarraga, F.; De Tovar, J.; Guerrero, M.; Nolis, P.; Parella, T.; Lecante, P.; Romero, N.; Escriche, L.; Bofill, R.; Ros, J.; et al. Dissimilar catalytic behavior of molecular or colloidal palladium systems with a new NHC ligand. *Dalton Trans.* **2017**, *46*, 11768–11778. [[CrossRef](#)]
12. Costa, N.J.S.; Guerrero, M.; Collière, V.; Teixeira-Neto, É.; Landers, R.; Philippot, K.; Rossi, L.M. Organometallic Preparation of Ni, Pd, and NiPd Nanoparticles for the Design of Supported Nanocatalysts. *ACS Catal.* **2014**, *4*, 1735–1742. [[CrossRef](#)]
13. Nie, W.; Luo, Y.; Yang, Q.; Feng, G.; Yao, Q.; Lu, Z.-H. An amine-functionalized mesoporous silica-supported PdIr catalyst: Boosting room-temperature hydrogen generation from formic acid. *Inorg. Chem. Front.* **2020**, *7*, 709–717. [[CrossRef](#)]
14. Zhang, Z.; Luo, Y.; Liu, S.; Yao, Q.; Qing, S.; Lu, Z.-H. A PdAg–CeO₂ nanocomposite anchored on mesoporous carbon: A highly efficient catalyst for hydrogen production from formic acid at room temperature. *J. Mater. Chem. A* **2019**, *7*, 21438–21446. [[CrossRef](#)]
15. Peng, W.; Liu, S.; Li, X.; Feng, G.; Xia, J.; Lu, Z.-H. Robust hydrogen production from HCOOH over amino-modified KIT-6-confined PdIr alloy nanoparticles. *Chin. Chem. Lett.* **2022**, *33*, 1403–1406. [[CrossRef](#)]
16. Sharma, A.K.; Joshi, H.; Bhaskar, R.; Singh, A.K. Solvent-tailored Pd₃P_{0.95} nano catalyst for amide–nitrile inter-conversion, the hydration of nitriles and transfer hydrogenation of the C=O bond. *Dalton Trans.* **2019**, *48*, 10962–10970. [[CrossRef](#)]
17. Singh, P.; Singh, A.K. Palladium(II) complexes of N,N-diphenylacetamide based thio/selenoethers and flower shaped Pd₁₆S₇ and prismatic Pd₁₇Se₁₅ nano-particles tailored as catalysts for C–C and C–O coupling. *Dalton Trans.* **2017**, *46*, 10037–10049. [[CrossRef](#)]
18. Arora, A.; Oswal, P.; Rao, G.K.; Kumar, S.; Singh, A.K.; Kumar, A. Catalytically active nanosized Pd₉Te₄ (telluropalladinite) and PdTe (kotulskite) alloys: First precursor-architecture controlled synthesis using palladium complexes of organotellurium compounds as single source precursors. *RSC Adv.* **2021**, *11*, 7214–7224. [[CrossRef](#)]

19. Vázquez-Céspedes, S.; Betori, R.C.; Cismesia, M.A.; Kirsch, J.K.; Yang, Q. Heterogeneous Catalysis for Cross-Coupling Reactions: An Underutilized Powerful and Sustainable Tool in the Fine Chemical Industry? *Org. Process. Res. Dev.* **2021**, *25*, 740–753. [[CrossRef](#)]
20. Wang, J.; Xu, F.; Jin, H.; Chen, Y.; Wang, Y. Non-Noble Metal-based Carbon Composites in Hydrogen Evolution Reaction: Fundamentals to Applications. *Adv. Mater.* **2017**, *29*, 1605838. [[CrossRef](#)]
21. Sultan, S.; Tiwari, J.N.; Singh, A.N.; Zhumagali, S.; Ha, M.; Myung, C.W.; Thangavel, P.; Kim, K.S. Single Atoms and Clusters Based Nanomaterials for Hydrogen Evolution, Oxygen Evolution Reactions, and Full Water Splitting. *Adv. Energy Mater.* **2019**, *9*, 1900624. [[CrossRef](#)]
22. Li, Z.; Ji, S.; Liu, Y.; Cao, X.; Tian, S.; Chen, Y.; Niu, Z.; Li, Y. Well-Defined Materials for Heterogeneous Catalysis: From Nanoparticles to Isolated Single-Atom Sites. *Chem. Rev.* **2020**, *120*, 623–682. [[CrossRef](#)] [[PubMed](#)]
23. Zalesskiy, S.S.; Ananikov, V.P. Pd₂(dba)₃ as a Precursor of Soluble Metal Complexes and Nanoparticles: Determination of Palladium Active Species for Catalysis and Synthesis. *Organometallics* **2012**, *31*, 2302–2309. [[CrossRef](#)]
24. Axet, M.R.; Dechy-Cabaret, O.; Durand, J.; Gouygou, M.; Serp, P. Coordination chemistry on carbon surfaces. *Coord. Chem. Rev.* **2016**, *308*, 236–345. [[CrossRef](#)]
25. Bourouina, A.; Meille, V.; de Bellefon, C. About Solid Phase vs. Liquid Phase in Suzuki-Miyaura Reaction. *Catalysts* **2019**, *9*, 60. [[CrossRef](#)]
26. Pagliaro, M.; Pandarus, V.; Ciriminna, R.; Béland, F.; Demma Carà, P. Heterogeneous versus Homogeneous Palladium Catalysts for Cross-Coupling Reactions. *Chemcatchem* **2012**, *4*, 432–445. [[CrossRef](#)]
27. Prima, D.O.; Kulikovskaya, N.S.; Galushko, A.S.; Mironenko, R.M.; Ananikov, V.P. Transition metal ‘cocktail’-type catalysis. *Curr. Opin. Green Sustain. Chem.* **2021**, *31*, 100502. [[CrossRef](#)]
28. Crabtree, R.H. Resolving Heterogeneity Problems and Impurity Artifacts in Operationally Homogeneous Transition Metal Catalysts. *Chem. Rev.* **2012**, *112*, 1536–1554. [[CrossRef](#)]
29. Eremin, D.B.; Ananikov, V.P. Understanding active species in catalytic transformations: From molecular catalysis to nanoparticles, leaching, “Cocktails” of catalysts and dynamic systems. *Coord. Chem. Rev.* **2017**, *346*, 2–19. [[CrossRef](#)]
30. Avanthay, M.; Bedford, R.B.; Begg, C.S.; Böse, D.; Clayden, J.; Davis, S.A.; Eloi, J.-C.; Goryunov, G.P.; Hartung, I.V.; Heeley, J.; et al. Identifying palladium culprits in amine catalysis. *Nat. Catal.* **2021**, *4*, 994–998. [[CrossRef](#)]
31. Widegren, J.A.; Finke, R.G. A review of the problem of distinguishing true homogeneous catalysis from soluble or other metal-particle heterogeneous catalysis under reducing conditions. *J. Mol. Catal. A Chem.* **2003**, *198*, 317–341. [[CrossRef](#)]
32. Kashin, A.S.; Ananikov, V.P. Catalytic C–C and C–Heteroatom Bond Formation Reactions: In Situ Generated or Preformed Catalysts? Complicated Mechanistic Picture Behind Well-Known Experimental Procedures. *J. Org. Chem.* **2013**, *78*, 11117–11125. [[CrossRef](#)]
33. Ananikov, V.P.; Orlov, N.V.; Zalesskiy, S.S.; Beletskaya, I.P.; Khrustalev, V.N.; Morokuma, K.; Musaev, D.G. Catalytic Adaptive Recognition of Thiol (SH) and Selenol (SeH) Groups Toward Synthesis of Functionalized Vinyl Monomers. *J. Am. Chem. Soc.* **2012**, *134*, 6637–6649. [[CrossRef](#)]
34. Yang, X.; Liu, W.; Tan, F.; Zhang, Z.; Chen, X.; Liang, T.; Wu, C. A robust strategy of homogeneously hybridizing silica and Cu₃(BTC)₂ to in situ synthesize highly dispersed copper catalyst for furfural hydrogenation. *Appl. Catal. A* **2020**, *596*, 117518. [[CrossRef](#)]
35. Qian, W.; Lin, L.; Qiao, Y.; Zhao, X.; Xu, Z.; Gong, H.; Li, D.; Chen, M.; Huang, R.; Hou, Z. Ru subnanoparticles on N-doped carbon layer coated SBA-15 as efficient Catalysts for arene hydrogenation. *Appl. Catal. A* **2019**, *585*, 117183. [[CrossRef](#)]
36. Beletskaya, I.P.; Cheprakov, A.V. The Heck Reaction as a Sharpening Stone of Palladium Catalysis. *Chem. Rev.* **2000**, *100*, 3009–3066. [[CrossRef](#)]
37. Kashin, A.N.; Ganina, O.G.; Cheprakov, A.V.; Beletskaya, I.P. The Direct Non-Perturbing Leaching Test in the Phosphine-Free Suzuki-Miyaura Reaction Catalyzed by Palladium Nanoparticles. *Chemcatchem* **2015**, *7*, 2113–2121. [[CrossRef](#)]
38. Sigeev, A.S.; Peregodov, A.S.; Cheprakov, A.V.; Beletskaya, I.P. The Palladium Slow-Release Pre-Catalysts and Nanoparticles in the “Phosphine-Free” Mizoroki-Heck and Suzuki-Miyaura Reactions. *Adv. Synth. Catal.* **2015**, *357*, 417–429. [[CrossRef](#)]
39. Beletskaya, I.P.; Alonso, F.; Tyurin, V. The Suzuki-Miyaura reaction after the Nobel prize. *Coord. Chem. Rev.* **2019**, *385*, 137–173. [[CrossRef](#)]
40. Beletskaya, I.; Tyurin, V. Recyclable Nanostructured Catalytic Systems in Modern Environmentally Friendly Organic Synthesis. *Molecules* **2010**, *15*, 4792–4814. [[CrossRef](#)]
41. Trzeciak, A.M.; Augustyniak, A.W. The role of palladium nanoparticles in catalytic C–C cross-coupling reactions. *Coord. Chem. Rev.* **2019**, *384*, 1–20. [[CrossRef](#)]
42. Trzeciak, A.M.; Ziółkowski, J.J. Monomolecular, nanosized and heterogenized palladium catalysts for the Heck reaction. *Coord. Chem. Rev.* **2007**, *251*, 1281–1293. [[CrossRef](#)]
43. Baumann, C.G.; De Ornellas, S.; Reeds, J.P.; Storr, T.E.; Williams, T.J.; Fairlamb, I.J.S. Formation and propagation of well-defined Pd nanoparticles (PdNPs) during C–H bond functionalization of heteroarenes: Are nanoparticles a moribund form of Pd or an active catalytic species? *Tetrahedron* **2014**, *70*, 6174–6187. [[CrossRef](#)]
44. Reay, A.J.; Fairlamb, I.J.S. Catalytic C–H bond functionalisation chemistry: The case for quasi-heterogeneous catalysis. *Chem. Commun.* **2015**, *51*, 16289–16307. [[CrossRef](#)]

45. Ellis, P.J.; Fairlamb, I.J.S.; Hackett, S.F.J.; Wilson, K.; Lee, A.F. Evidence for the Surface-Catalyzed Suzuki-Miyaura Reaction over Palladium Nanoparticles: An Operando XAS Study. *Angew. Chem. Int. Ed. Engl.* **2010**, *49*, 1820–1824. [[CrossRef](#)] [[PubMed](#)]
46. Scott, N.W.J.; Ford, M.J.; Schotes, C.; Parker, R.R.; Whitwood, A.C.; Fairlamb, I.J.S. The ubiquitous cross-coupling catalyst system 'Pd(OAc)₂/2PPh₃' forms a unique dinuclear Pd^I complex: An important entry point into catalytically competent cyclic Pd₃ clusters. *Chem. Sci.* **2019**, *10*, 7898–7906. [[CrossRef](#)]
47. Fairlamb, I.J.S. Redox-Active NO_x Ligands in Palladium-Mediated Processes. *Angew. Chem. Int. Ed. Engl.* **2015**, *54*, 10415–10427. [[CrossRef](#)]
48. Zhao, F.; Shirai, M.; Arai, M. Palladium-catalyzed homogeneous and heterogeneous Heck reactions in NMP and water-mixed solvents using organic, inorganic and mixed bases. *J. Mol. Catal. A Chem.* **2000**, *154*, 39–44. [[CrossRef](#)]
49. Zhao, F.; Murakami, K.; Shirai, M.; Arai, M. Recyclable Homogeneous/Heterogeneous Catalytic Systems for Heck Reaction through Reversible Transfer of Palladium Species between Solvent and Support. *J. Catal.* **2000**, *194*, 479–483. [[CrossRef](#)]
50. Cantillo, D.; Kappe, C.O. Immobilized Transition Metals as Catalysts for Cross-Couplings in Continuous Flow—A Critical Assessment of the Reaction Mechanism and Metal Leaching. *Chemcatchem* **2014**, *6*, 3286–3305. [[CrossRef](#)]
51. Huo, J.; Tessonnier, J.-P.; Shanks, B.H. Improving Hydrothermal Stability of Supported Metal Catalysts for Biomass Conversions: A Review. *ACS Catal.* **2021**, *11*, 5248–5270. [[CrossRef](#)]
52. Otor, H.O.; Steiner, J.B.; García-Sancho, C.; Alba-Rubio, A.C. Encapsulation Methods for Control of Catalyst Deactivation: A Review. *ACS Catal.* **2020**, *10*, 7630–7656. [[CrossRef](#)]
53. Galushko, A.S.; Gordeev, E.G.; Kashin, A.S.; Zubavichus, Y.V.; Ananikov, V.P. Visualization of catalyst dynamics and development of a practical procedure to study complex “cocktail”-type catalytic systems. *Faraday Discuss.* **2021**, *229*, 458–474. [[CrossRef](#)]
54. Fulignati, S.; Antonetti, C.; Licursi, D.; Pieraccioni, M.; Wilbers, E.; Heeres, H.J.; Galletti, A.M.R. Insight into the hydrogenation of pure and crude HMF to furan diols using Ru/C as catalyst. *Appl. Catal. A* **2019**, *578*, 122–133. [[CrossRef](#)]
55. Novák, Z.; Szabó, A.; Répási, J.; Kotschy, A. Sonogashira Coupling of Aryl Halides Catalyzed by Palladium on Charcoal. *J. Org. Chem.* **2003**, *68*, 3327–3329. [[CrossRef](#)]
56. Köhler, K.; Heidenreich, R.G.; Soomro, S.S.; Pröckl, S.S. Supported Palladium Catalysts for Suzuki Reactions: Structure-Property Relationships, Optimized Reaction Protocol and Control of Palladium Leaching. *Adv. Synth. Catal.* **2008**, *350*, 2930–2936. [[CrossRef](#)]
57. Salamatmanesh, A.; Heydari, A. Magnetic nanostructure-anchored mixed-donor ligand system based on carboxamide and N-heterocyclic thiones: An efficient support of CuI catalyst for synthesis of imidazo[1,2-a]pyridines in eutectic medium. *Appl. Catal. A* **2021**, *624*, 118306. [[CrossRef](#)]
58. Nikoshvili, L.; Bakhvalova, E.S.; Bykov, A.V.; Sidorov, A.I.; Vasiliev, A.L.; Matveeva, V.G.; Sulman, M.G.; Sapunov, V.N.; Kiwi-Minsker, L. Study of Deactivation in Suzuki Reaction of Polymer-Stabilized Pd Nanocatalysts. *Processes* **2020**, *8*, 1653. [[CrossRef](#)]
59. Xu, Z.; Li, M.; Shen, G.; Chen, Y.; Lu, D.; Ren, P.; Jiang, H.; Wang, X.; Dai, B. Solvent Effects in the Preparation of Catalysts Using Activated Carbon as a Carrier. *Nanomaterials* **2023**, *13*, 393. [[CrossRef](#)]
60. Yakukhnov, S.A.; Pentsak, E.O.; Galkin, K.I.; Mironenko, R.M.; Drozdov, V.A.; Likholobov, V.A.; Ananikov, V.P. Rapid “Mix-and-Stir” Preparation of Well-Defined Palladium on Carbon Catalysts for Efficient Practical Use. *Chemcatchem* **2017**, *10*, 1869–1873. [[CrossRef](#)]
61. Liu, X.; Astruc, D. Development of the Applications of Palladium on Charcoal in Organic Synthesis. *Adv. Synth. Catal.* **2018**, *360*, 3426–3459. [[CrossRef](#)]
62. Pentsak, E.O.; Eremin, D.B.; Gordeev, E.G.; Ananikov, V.P. Phantom Reactivity in Organic and Catalytic Reactions as a Consequence of Microscale Destruction and Contamination-Trapping Effects of Magnetic Stir Bars. *ACS Catal.* **2019**, *9*, 3070–3081. [[CrossRef](#)]
63. Galushko, A.S.; Boiko, D.A.; Pentsak, E.O.; Eremin, D.B.; Ananikov, V.P. Time-Resolved Formation and Operation Maps of Pd Catalysts Suggest a Key Role of Single Atom Centers in Cross-Coupling. *J. Am. Chem. Soc.* **2023**, *145*, 9092–9103. [[CrossRef](#)] [[PubMed](#)]
64. Nishchakova, A.D.; Bulusheva, L.G.; Bulushev, D.A. Supported Ni Single-Atom Catalysts: Synthesis, Structure, and Applications in Thermocatalytic Reactions. *Catalysts* **2023**, *13*, 845. [[CrossRef](#)]
65. Wang, A.; Li, J.; Zhang, T. Heterogeneous single-atom catalysis. *Nat. Rev. Chem.* **2018**, *2*, 65–81. [[CrossRef](#)]
66. Li, Z.; Hong, R.; Zhang, Z.; Wang, H.; Wu, X.; Wu, Z. Single-Atom Catalysts in Environmental Engineering: Progress, Outlook and Challenges. *Molecules* **2023**, *28*, 3865. [[CrossRef](#)]
67. Teipel, J.; Gottstein, V.; Hölzle, E.; Kaltenbach, K.; Lachenmeier, D.; Kuballa, T. An Easy and Reliable Method for the Mitigation of Deuterated Chloroform Decomposition to Stabilise Susceptible NMR Samples. *Chemistry* **2022**, *4*, 776–785. [[CrossRef](#)]
68. Dann, E.K.; Gibson, E.K.; Blackmore, R.H.; Catlow, C.R.A.; Collier, P.; Chutia, A.; Erden, T.E.; Hardacre, C.; Kroner, A.; Nachttegaal, M.; et al. Structural selectivity of supported Pd nanoparticles for catalytic NH₃ oxidation resolved using combined operando spectroscopy. *Nat. Catal.* **2019**, *2*, 157–163. [[CrossRef](#)]
69. Chatterjee, A.; Ward, T.R. Recent Advances in the Palladium Catalyzed Suzuki–Miyaura Cross-Coupling Reaction in Water. *Catal. Lett.* **2016**, *146*, 820–840. [[CrossRef](#)]
70. Ding, S.; Jiao, N. Direct Transformation of *N,N*-Dimethylformamide to –CN: Pd-Catalyzed Cyanation of Heteroarenes via C–H Functionalization. *J. Am. Chem. Soc.* **2011**, *133*, 12374–12377. [[CrossRef](#)]

71. Yang, X.-F.; Wang, A.; Qiao, B.; Li, J.; Liu, J.; Zhang, T. Single-Atom Catalysts: A New Frontier in Heterogeneous Catalysis. *Acc. Chem. Res.* **2013**, *46*, 1740–1748. [[CrossRef](#)]
72. Markov, P.V.; Bragina, G.O.; Smirnova, N.S.; Baeva, G.N.; Mashkovsky, I.S.; Gerasimov, E.Y.; Bukhtiyarov, A.V.; Zubavichus, Y.V.; Stakheev, A.Y. Single-Atom Alloy Pd₁Ag₁₀/CeO₂–ZrO₂ as a Promising Catalyst for Selective Alkyne Hydrogenation. *Inorganics* **2023**, *11*, 150. [[CrossRef](#)]
73. Chen, Z.; Vorobyeva, E.; Mitchell, S.; Fako, E.; Ortuño, M.A.; López, N.; Collins, S.M.; Midgley, P.A.; Richard, S.; Vilé, G.; et al. A heterogeneous single-atom palladium catalyst surpassing homogeneous systems for Suzuki coupling. *Nat. Nanotechnol.* **2018**, *13*, 702–707. [[CrossRef](#)]
74. Eremin, D.B.; Galushko, A.S.; Boiko, D.A.; Pentsak, E.O.; Chistyakov, I.V.; Ananikov, V.P. Toward Totally Defined Nanocatalysis: Deep Learning Reveals the Extraordinary Activity of Single Pd/C Particles. *J. Am. Chem. Soc.* **2022**, *144*, 6071–6079. [[CrossRef](#)]

Disclaimer/Publisher’s Note: The statements, opinions and data contained in all publications are solely those of the individual author(s) and contributor(s) and not of MDPI and/or the editor(s). MDPI and/or the editor(s) disclaim responsibility for any injury to people or property resulting from any ideas, methods, instructions or products referred to in the content.